# Interplay of electronic, magnetic and structural properties of surface-supported clusters

P.A. Ignatiev[1,a], V.S. Stepanyuk[1], L. Niebergall[1], P. Bruno[1], and J. Berakdar[2]

[1] Max-Planck-Institut für Mikrostrukturphysik, Weinberg 2, 06120 Halle, Germany
[2] Institut für Physik, Martin-Luther-Universität Halle-Wittenberg, Nanotechnikum-Weinberg, Heinrich-Damerow-Str. 4, 06120 Halle, Germany

**Abstract.** We present first theoretical evidence revealing the influence of structural changes on the spin-polarized surface states of large Co nanoislands grown on Cu(111). The minority density of electronic states possesses a pronounced peak whose energetic position depends sensitively on the Co layers stacking order. Our results suggest a way to deduce the stacking order of large Co nanoislands using scanning tunnelling microscopy/spectroscopy.

**PACS.** 73.20.-r Electron states at surfaces and interfaces – 73.20.At Surface states, band structure, electron density of states – 73.22.-f Electronic structure of nanoscale materials: clusters, nanoparticles, nanotubes, and nanocrystals

## 1 Introduction

The impressive progress in engineering, imaging and control of nanostructures have revealed a wealth of fascinating phenomena. E.g., experiments by Manoharan et al. [1] revealed how the electronic structure of an adatom is projected onto a remote location when placed in a quantum corral: depositing a cobalt atom at one focus of an elliptical corral built out of other cobalt atoms on a Cu(111) surface results in a Kondo mirage at the empty focus. The physical mechanisms underlying this phenomena have been discussed by a number of theoretical studies [1–5]. Our contribution has been to undertake first-principle calculations [6,7] that delivered a quantitative understanding and allowed the investigation of the various dependencies of quantum-interference effects on real material parameters and geometrical arrangement of the confinement. For instance, one of our findings is that the exchange interaction in the corral is strongly enhanced compared to an open surface and hence the modification of the corral geometry allows a switching from a ferromagnetic coupling to an antiferromagnetic one. Vacancy holes on Cu(111) [7] acting as natural quantum resonators are also an exciting possibility for inspecting confinement-induced effects.

Spin-polarized surface states arising on magnetic nanostructures supported on nonmagnetic substrates (e.g. Co islands on Cu(111)) have attracted much attention recently [9,10,12,14]. Spin-polarized surface-state (SP-SS) may act as spin-dependent channels for transport to or from another magnetic material [11]. We demonstrated that the SP-SS can be controlled to a large degree by an appropriate modulation of the nanostructure geometry [12]. Concrete numerical and analytical calculations have endorsed that the spin-polarization at $E_F$ of two Co monolayers on Cu(111) is changeable locally and energetically if Cu corrals or triangular Co islands are deposited on top [12]. These findings are meanwhile experimentally confirmed [14].

Another related topic of research concerns the mechanisms of nanostructures growth driven by quantum confinement of surface-state electrons. The question is most suitably addressed by means of ab initio calculations (for the steady-state energetic of the system) and (classical) kinetic Monte Carlo (kMC) simulations for the description of the confinement-induced adatom self-organization kinetics. Our conclusion is that self-organized new types of magnetic nanostructures appear during low-temperature deposition of atoms onto quantum resonators (corrals, vacancy holes and nanoislands) [15]. In addition, it has been shown that the diffusion of an adatom confined to a corral is markedly different from that occurring on an open surface [15]. Our studies allow to conclude that atomic self-organization in corrals is governed by a delicate balance of the adatom diffusion barrier, the sample temperature, and the adatom concentration. Experimentally, it has been shown recently that Ce adatoms on Ag(111) form a 2D hexagonal superlattice with a lattice constant of 32 Å [17]. Our kMC investigations have revealed the mechanism of the superlattice formation [16]. To study

[a] e-mail: `ignatiev@mpi-halle.de`

the effect of quantum confinement of surface electrons on atomic motion we assumed Ce adatoms randomly deposited inside the corral made of Ce dimers on Ag(111). The self-organization of Ce adatoms resulted in different concentric circular orbits that form a 'quantum onion' shape structure [15]. A further issue related to cluster growth and structure is the atomic relaxations of supported clusters which turned out to be determined by the size-dependent mismatch [18]. The findings are that small clusters on metal surfaces exhibit strong atomic relaxations at their edges [19]. Also the substrate experiences a significant atomic relaxations due to the interaction with a deposited cluster [18,19].

In this work we draw attention to the decisive influence of structural properties of the Co nanoislands grown on Cu(111) on the spin-polarized surface states. By means of ab-initio methods we demonstrate a possible way to link the scanning tunnelling microscopy/spectroscopy (STM/STS) data with a stacking order of large islands.

## 2 Theoretical framework

The details of our calculational scheme have been described in a number of publications [6–8]. Hence, here we give only a brief sketch. The method rests on the density functional theory (DFT) combined with the multiple-scattering-based Korringa-Kohn-Rostoker (KKR) Green's function method. First, the surface is treated as a 2D perturbation of the bulk so it is possible to write down and self consistently solve the 2D Dyson equation. Then, if we want to calculate adatoms and clusters on surfaces, the Green's function of the cluster is determined in a real space representation, i.e.

$$G_{LL'}^{nn'}(E) = \mathring{G}_{LL'}^{nn'}(E) + \sum_{n''L''} \mathring{G}_{LL''}^{nn''}(E) \Delta t_{L''}^{n''}(E) G_{L''L'}^{n''n'}(E).$$

Here $G_{LL'}^{nn'}(E)$ is the energy-dependent structural Green's function matrix and $\mathring{G}_{LL''}^{nn''}(E)$ is the reference matrix for the ideal surface. $\Delta t_L^n(E)$ is the difference in the scattering properties at site $n$ induced by the existence of the cluster and adatoms.

Relaxation is an issue deserving careful attention. Large strain relaxations in clusters may affect decisively the magnetic moments in clusters and the magnetic anisotropy energy (MAE) [19]. Our way to deal with this problem is to use ab-initio based interatomic potentials formulated in the second-moment approximation of the tight-binding theory and the tight-binding approach for the calculations of magnetic properties [20]. To determine the parameters of the potentials we use a fitting to the ab initio KKR Green's function results [20] for surface properties. The interaction between atoms near the surface and in bulk is accounted for in that the set of data used for the fitting includes bulk properties (bulk modulus, lattice constant, cohesive energy and elastic constants). The full potential approximation is used in the calculations of the Hellmann-Feynman (HF) forces. Tests

have been performed [21] to ensure the quality of the interatomic potentials.

## 3 Interplay between structural properties and spin-polarized surface states

Ultrathin cobalt films on noble metals substrates have recently been in the focus of of numerous investigations [9,10,12,14,22,23]. One of the fundamental questions under consideration is the relation between structure and electronic properties of such low-dimensional nanostructures [10,14,22]. In the most simple case when lattice mismatch between Co and the substrate is small, structural changes are determined by different stacking order of the Co film layers, as it is for Co islands on Cu(111) substrate [10]. A large lattice mismatch leads to a reconstruction in Co structures: layer-high Co islands on Pt(111) consist of fcc and hcp stacking regions separated by Co atoms in the bridge site positions [22]. The herringbone reconstruction of Au(111) provides areas of fcc and hcp stackings for Co nucleation [23]. An adequate treatment of such complicated reconstructions by means of ab-initio methods must involve hundreds of inequivalent atoms. As such calculations require extensive computational resources, differently stacked monolayers are usually used to investigate surface states on the corresponding region of the reconstructed surface. An example is the recent study of Co on Pt(111) [22] and Co on Au(111) [23]. Good agreement of the obtained results with scanning tunnelling spectroscopy/microscopy (STS/STM) data indicates the value of this approximation in reproducing the main properties of the studied system.

Surface states of unfaulted Co islands grown in fcc stacking order on Cu(111) substrate have already been studied both experimentally and theoretically [9,10,14] with the following conclusions: a sharp peak in the density of state situated at −0.31 eV below $E_F$ and a mainly unoccupied dispersive state have been observed [9,10]. The peak is formed by the minority states whereas the dispersive states are of a majority character and possess parabolic dispersion. This spin-splitting and the delocalized nature of the majority states result in a spatially varying polarization across the islands [12]; a theoretical prediction that has been confirmed recently by means of spin-polarized spectroscopic techniques [14]. In addition, experimental evidence indicates a dependence of the surface states above the Co islands on the islands structure. STS measurements performed on the faulted Co islands shows that the minority peak is situated closer to the Fermi energy than that measured on the unfaulted ones [10]. Even though the surface states on Co islands deposited on Cu(111) have been investigated in detail, to the best of our knowledge no theoretical studies exist on the interplay between the stacking order of the Co ultrathin films grown on a Cu(111) substrate and the electronic properties. The aim here is to fill this gap by means of ab-initio calculations.

At room temperature, evaporated Co adatoms form triangular islands that are two monolayers in height and
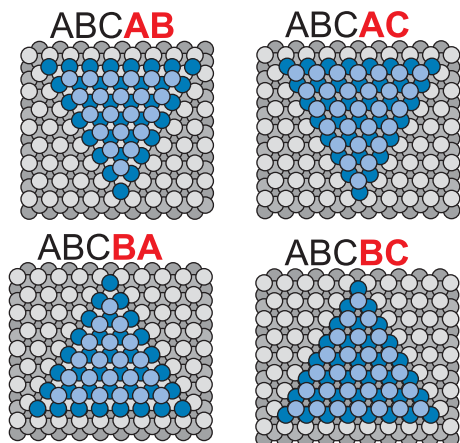
**Fig. 1.** (Color online) Four possible stacking orders of Co bilayer on a Cu(111) substrate shown with respect to the triangular island orientation. Letter sequences stand for the stacking order.



**Fig. 2.** (Color online) The LDOS calculated above differently stacked Co bilayers. The shift of the main peak is clearly visible.



**Fig. 3.** (Color online) Spectral density map calculated above the topmost Co layer of fcc-stacked structure at the energy of the main peak ($E = -0.47$ eV). The main contribution to the peak gives a ring marked with the red circle.

oriented in opposite directions on a Cu(111) substrate [24–26]. According to Ovesson et al. [27] the triangles are formed due to the anisotropic diffusion barriers at island corners. At room temperature, adatoms jump easily from the A step (the step with {100} facet) to B step (the step with {111} facet). A reverse motion from B step to A is less probable than a further diffusion along the B step [26]. As a result, the length of the B steps decreases until only one atom is left. Such a scenario suggests that the first layer of the Co triangular islands on Cu(111) always forms the B step and therefore, different orientations of the Co islands are a signature of a stacking fault. Here we assume that the second Co layer can grow both on fcc and hcp sites simply filling the area of the first layer.

Differently stacked Co bilayer islands with respect to their orientations are sketched in Figure 1. A stacking order is noted by the letter sequence. The first 3 letters ABC stand for the *fcc* stacking order of Cu(111) substrate. The last two letters show the stacking order of the Co layers. As it has been already mentioned, in our calculations we consider large Co islands as infinite layers stacked in an appropriate way. The LDOS calculated above the topmost Co layer are shown in Figure 2 for all possible stacking orders. The main peak reported by Diekhöner et al. [9] is clearly visible but its exact position significantly depends on the Co layers stacking: ABCAB and ABCBA stackings yield the peak at $-0.47$ eV and ABCBC and ABCAC result in the peak at $-0.40$ eV [10]. It should be noted that a pair of oppositely oriented islands corresponds to each peak position and therefore it is possible to deduce the stacking order of large islands from the island orientation and spectral information. Our investigations have not revealed the dependence of the majority states upon the Co bilayer stacking. For all considered stackings, majority surface states are free-electron like with the same parabolic dispersion.

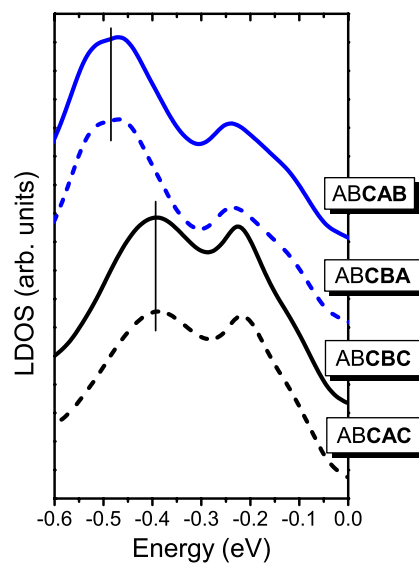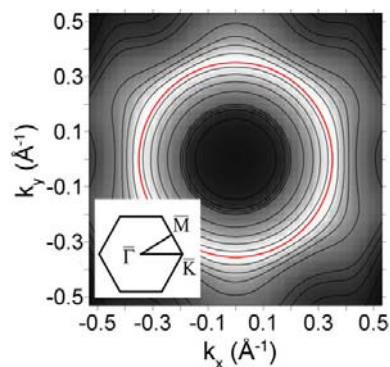For a deeper insight into the problem we discuss the origin of the minority peak with the aim to consider the origin of the sensitivity of the peak positions to structural changes. As a test system we choose *fcc*-stacked (ABCAB) Co bilayer. The momentum-resolved spectral density map (SDM) calculated above the topmost Co layer at the peak energy of $-0.47$ eV is displayed in Figure 3. The main contribution to the peak gives a ring which is highlighted in Figure 3 with the red circle. The ring has a finite width near the $\Gamma$-M lines. Our calculations demonstrated that in the vacuum the peak is formed by strongly hybridized *s-p-d* states. For a detailed understanding we investigated the SDM underneath Co and Cu layers. The hybridized states arise at the Cu-Co interface due to hybridization of Cu *s-p* states with *d*-states of Co bilayer. For an illustration we plot in Figure 4a SDM of the interface Cu layer. A wide grey area at the right side of the figure is Cu bulk band. Bright stripes are bands determined by Co-Cu hybridized *d*-bands. Area contributing to the main peak is marked in Figure 4 with the red oval. It can be directly compared with the SDM calculated above the topmost Co layer (see
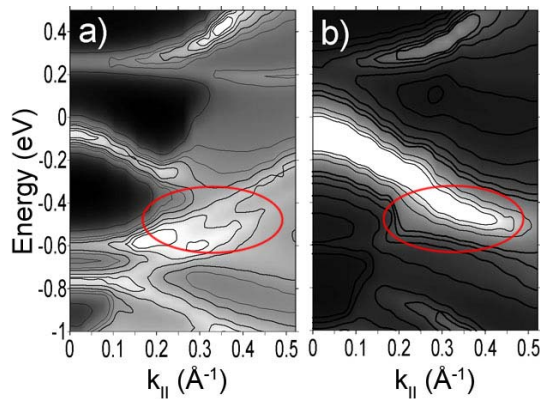
**Fig. 4.** (Color online) Momentum-resolved spectral density map (SDM) of: (a) the interface Cu layer, and (b) in the vacuum above the topmost Co layer calculated along the $\Gamma$-M direction. A wide grey area at the left side of (a) is Cu bulk band and bright stripes are bands originating from the Cu-Co hybridization. The area contributing to the main peak is marked with the red oval line.



**Fig. 5.** (Color online) The LDOS calculated above differently stacked Co trilayers. Four different positions of the main peak exist.

Fig. 4b). For differently stacked Co bilayers Co-Cu hybridization occurs at different energies and therefore the position of the surface-states minority peak also shifts. In principle, the peak position should be different for all the stacking orders, even though in practice we observe only two pronounced positions. This can be rationalized in the following way: one should consider that only the coupling between Co layers and the interface Cu layer is important. There are two general ways to attach a Co bilayer to the Cu(111) surface: (i) the interface Cu and two Co layers form *fcc*-like layer sequences CAB and CBA; (ii) the topmost three layers are stacked *hcp*-like (sequences CBC and CAC). Two peak positions ($-0.47$ eV and $-0.40$ eV) demonstrated in Figure 2 are produced by the structures which are symmetrical and hence equivalent. This idea can be extended to the situation of three Co layers placed on Cu(111). In this case 8 different ways to stack Co layers on the fcc substrate do exist. The LDOS's calculated above such structures are plotted in Figure 5. It is evident that there are 4 different positions of the peak situated between $-0.45$ eV and $-0.40$ eV.

It is important to note here that the position of the minority peak depends significantly on the substrate lattice constant and hence on the lateral distances between Co atoms [23]. In particular, Co bilayer on Cu(111) substrate expanded to the Au lattice constant gives peak positions significantly shifted to $E_F$, similar to natural Co2ML/Au(111) system.

## 4 Conclusions

We demonstrated explicitly the relation between the structure of Co islands on Cu(111) and their surface states by means of ab-initio calculations. Structural changes are found to affect significantly the positions of the pronounced surface-states minority-character peak below the
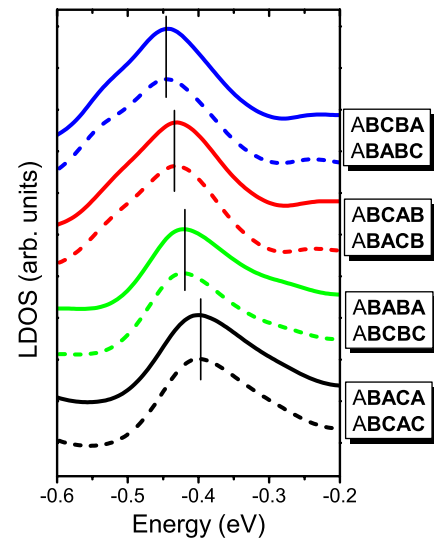
Fermi energy. This peak, formed by *s-p-d* hybridized surface states, arises from the coupling of Cu *s-p* states to the d-states of Co bilayer. Changing the stacking order of Co bilayer results in a shift of the d-states. As a consequence the peak position also shifts. From the above we conclude on the possibility to deduce the Co bilayer stacking order from STS/STM data exploiting the relationship between Co triangle island orientation, the peak position and the stacking order.

## References

1. H.C. Manoharan, C.P. Lutz, D.M. Eigler, Nature **403**, 512 (2000)
2. G.A. Fiete, J.S. Hersch, E.J. Heller, H.C. Manoharan, C.P. Lutz, D.M. Eigler, Phys. Rev. Lett. **86**, 2392 (2001)
3. O. Agam, A. Schiller, Phys. Rev. Lett. **86**, 484 (2001)
4. K. Hallberg, A.A. Correa, C.A. Balseiro, Phys. Rev. Lett. **88**, 066802 (2002); A. Correa, K. Hallberg, C.A. Balseiro, Europhys. Lett. **58**, 899 (2002)
5. D.K. Morr, N.A. Stavropoulos, Phys. Rev. Lett. **92**, 107006 (2004)
6. V.S. Stepanyuk, L. Niebergall, W. Hergert, P. Bruno, Phys. Rev. Lett. **94**, 187201 (2005)
7. L. Niebergall, G. Rodary, H.F. Ding, D. Sander, V.S. Stepanyuk, P. Bruno, J. Kirschner, Phys. Rev. B **74**, 195436 (2006)
8. K. Wildberger, V.S. Stepanyuk, P. Lang, R. Zeller, P.H. Dederichs, Phys. Rev. Lett. **75**, 509 (1995)
9. L. Diekhöner, M.A. Schneider, A.N. Baranov, V.S. Stepanyuk, P. Bruno, K. Kern, Phys. Rev. Lett. **90**, 236801 (2003)

10. O. Pietzsh, A. Kubetzka, M. Bode, R. Wiesendanger, Phys. Rev. Lett. **92**, 057202 (2004)
11. E.Y. Tsymbal, O.N. Mryasov, P.R. LeClair, J. Phys.: Condens. Matter **15**, R109 (2003)
12. L. Niebergall, V.S. Stepanyuk, J. Berakdar, P. Bruno, Phys. Rev. Lett. **96**, 127204 (2006)
13. A.L. Vázquez de Parga, F.J. García-Vidal, R. Miranda, Phys. Rev. Lett. **85**, 4365 (2000)
14. O. Pietzsch, S. Okatov, A. Kubetzka, M. Bode, S. Heinze, A. Lichtenstein, R. Wiesendanger, Phys. Rev. Lett. **96**, 237203 (2006)
15. V.S. Stepanyuk, N.N. Negulyaev, L. Niebergall, R.C. Longo, P. Bruno, Phys. Rev. Lett. **97**, 186403 (2006)
16. N.N. Negulyaev, V.S. Stepanyuk, L. Niebergall, W. Hergert, H. Fangohr, P. Bruno, Phys. Rev. B **74**, 035421 (2006)
17. F. Silly, M. Pivetta, M. Ternes, F. Patthey, J.P. Pelz, W.-D. Schneider, Phys. Rev. Lett. **92**, 016101 (2004)
18. V.S. Stepanyuk, D.I. Bazhanov, A.N. Baranov, W. Hergert, P.H. Dederichs, J. Kirschner, Phys. Rev. B **62**, 15398 (2000); O.V. Lysenko, V.S. Stepanyuk, W. Hergert, J. Kirschner, Phys. Rev. Lett. **89**, 126102 (2002)
19. Š. Pick, V.S. Stepanyuk, A.L. Klavsyuk, L. Niebergall, W. Hergert, J. Kirschner, P. Bruno, Phys. Rev. B **70**, 224419 (2004); Š. Pick, V.S. Stepanyuk, A.N. Baranov, W. Hergert, P. Bruno, Phys. Rev. B **68**, 104410 (2003)
20. N.A. Levanov, V.S. Stepanyuk, W. Hergert, D.I. Bazhanov, P.H. Dederichs, A. Katsnelson, C. Massobrio, Phys. Rev. B **61**, 2230 (2000)
21. V.S. Stepanyuk, A.L. Klavsyuk, L. Niebergall, A.M. Saletsky, W. Hergert, P. Bruno, Phase Tran. **78**, 61 (2005)
22. F. Meier, K. von Bergmann, P. Ferriani, J. Wiebe, M. Bode, K. Hashimoto, S. Heinze, R. Wiesendanger, Phys. Rev. B **74**, 195411 (2006)
23. M.V. Rastei, J.P. Bucher, P.A. Ignatiev, V.S. Stepanyuk, P. Bruno, Phys. Rev. B **75**, 045436 (2007)
24. J. de la Figuera, J.E. Prieto, C. Ocal, R. Miranda, Phys. Rev. B **47**, 13043 (1993)
25. M.Ø. Pedersen, I.A. Bönicke, E. Laegsgaard, I. Stensgaard, A. Ruban, J.K. Nørskov, F. Besenbacher, Surf. Sci. **387**, 86 (1997)
26. N.N. Negulaev et al. (unpublished)
27. S. Ovesson, A. Bogicevic, B.I. Lundqvist, Phys. Rev. Lett. **83**, 2608 (1999)